

## **YebC2 resolves ribosome stalling at polyprolines independent of EF-P and the ABCF ATPase YfmR**

Authors: Hye-Rim Hong<sup>1</sup>, Cassidy R. Prince<sup>1</sup>, Letian Wu<sup>1</sup>, Isabella N. Lin<sup>1</sup>, Heather A. Feaga<sup>1\*</sup>

Affiliations:

<sup>1</sup> Department of Microbiology, Cornell University, Ithaca, NY 14853

\* Corresponding author [haf54@cornell.edu](mailto:haf54@cornell.edu)

## Abstract

Polyproline motifs are essential structural features of many proteins, and recent evidence suggests that EF-P is one of several factors that facilitate their translation. For example, YfmR was recently identified as a protein that prevents ribosome stalling at proline-containing sequences in the absence of EF-P. Here, we show that the YebC-family protein YebC2 (formerly YeeI) functions as a translation factor in *B. subtilis* that resolves ribosome stalling at polyprolines. We demonstrate that YebC2, EF-P and YfmR act independently to support cellular fitness. Moreover, we show that YebC2 interacts directly with the 70S ribosome, supporting a direct role for YebC2 in translation. Finally, we assess the evolutionary relationship between YebC2 and other characterized YebC family proteins, and present evidence that transcription and translation factors within the YebC family have evolved separately. Altogether our work identifies YebC2 as a translation factor that resolves ribosome stalling and provides crucial insight into the relationship between YebC2, EF-P, and YfmR, three factors that prevent ribosome stalling at prolines.

## Introduction

Ribosomes catalyze peptide bond formation between amino acids to produce proteins. The polymerization rate is heavily influenced by the identity of the amino acids involved, with proline posing a special challenge due to its side chain forming a rigid pyrrolidine loop that limits flexibility of the peptide backbone in the ribosomal exit tunnel [1,2]. EF-P was the first protein shown to resolve ribosome stalling at polyprolines and other difficult-to-translation sequences [1,3–9]. EF-P interacts transiently with the ribosomal E-site and then binds stably when tRNA<sup>Pro</sup> is present in the P-site [10,11]. EF-P binding promotes a favorable geometry of the polypeptide in the exit tunnel to facilitate peptide bond formation [1,2]. *efp* is essential in *Mycobacterium tuberculosis*, *Acinetobacter baumannii*, and *Neisseria meningitidis* [12–14]. In contrast, *efp* deletion from *B. subtilis* causes sporulation and motility defects but does not cause a growth defect in standard lab conditions [15–19].

Recently, our group and Takada and colleagues identified YfmR as a protein that prevents ribosome stalling at polyproline tracts and Asp-Pro motifs in *Bacillus subtilis*, and which becomes more essential in the absence of EF-P [20,21]. YfmR is a member of the ABCF family of ATPases that are widespread throughout bacteria and eukaryotes and have diverse roles in preventing ribosome stalling and mediating antibiotic resistance [22–27]. The *Escherichia coli* homolog of YfmR, Uup, resolves ribosome stalling at polyprolines *in vitro* [28]. A recent structure of Uup bound to *E. coli* ribosomes reveals that it binds the ribosomal E-site and makes contacts with the peptidyl-transferase center [29,30], suggesting that YfmR/Uup may promote peptide bond formation in a manner similar to EF-P. In support of this model, deletion of *yfmR* or *efp* does not result in a fitness defect in *B. subtilis*, while deletion of *yfmR* and *efp* resulted in a severe synthetic fitness defect [21].

The screen we used to identify YfmR also uncovered *yebC2* (formerly *yeel*) as a gene that may be important for fitness in  $\Delta$ *efp* cells. Consistent with this finding, a screen performed by Hummels and colleagues in 2019 also identified *yebC2* (*yeel*) as a gene whose over-expression

could rescue the swarming motility defect of  $\Delta efp$  *B. subtilis* cells [18]. YebC family proteins are annotated as transcription factors in bacteria since these proteins exhibit promoter binding activity and *yebC* deletion causes differential gene expression in *E. coli*, *Pseudomonas aeruginosa*, *Lactobacillus delbrueckii* and in *Borrelia burgdorferi* [31–34]. The human YebC homolog, TACO1, is localized to mitochondria where it is important for efficient translation of COXI [35,36]. TACO1 was recently shown by mitoribosome profiling to prevent ribosome stalling at XPPX motifs and therefore accelerate translation of COXI in human cells [37] and recent work by Ignatov and colleagues demonstrates that YebC in *Streptococcus pyogenes* (YebC\_II) facilitates translation of polyproline motifs both *in vivo* and *in vitro* [38].

Here, we show that *B. subtilis* YebC2 is a translation factor that prevents ribosome stalling at a polyproline tract and determine its genetic interaction with *efp* and *yfmR*. Depleting EF-P from  $\Delta yebC2$  cells causes a severe fitness defect, and this defect is even more severe in  $\Delta yebC2\Delta yfmR$  cells, suggesting that EF-P, YfmR, and YebC2 function independently to support cellular fitness. We find that cells lacking both EF-P and YebC2 exhibit severe ribosome stalling at a polyproline track *in vivo* and that over-expression of YebC2 in  $\Delta efp$  cells reduces ribosome stalling. We show that YebC2 associates with 70S ribosomes, which suggests that YebC2 facilitates translation by acting directly on the ribosome. Finally, we present evidence that YebC2 proteins represent a class of translation factors that are evolutionarily distinct from the previously characterized YebC transcription factors.

## Results

### Deletion of *efp* and *yebC2* causes a severe growth defect and impaired protein synthesis

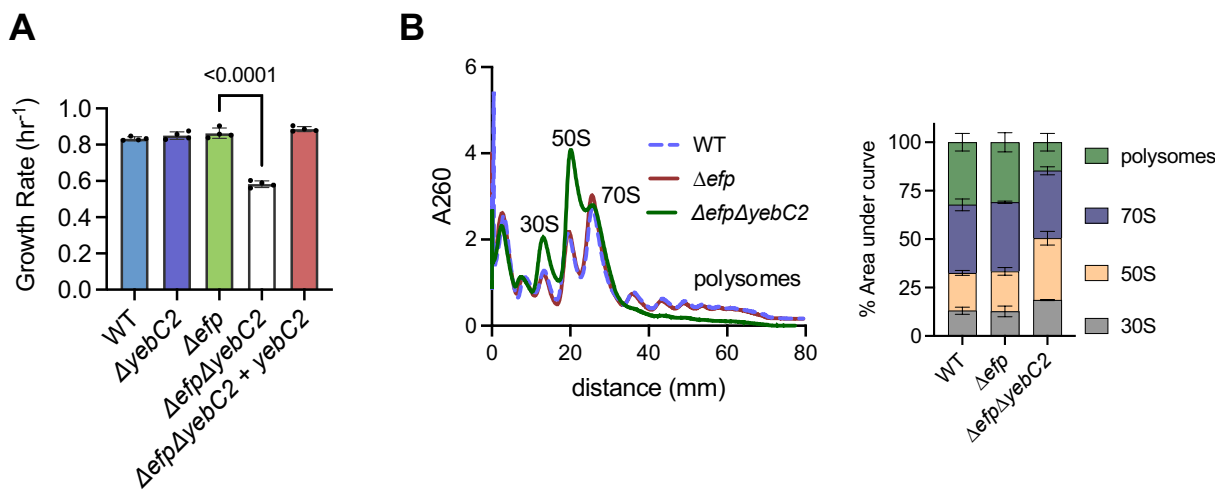
Previously, we investigated genetic interactions with *efp* using Tn-seq [20]. This screen predicted that *yfmR* is more essential in the absence of EF-P, and we confirmed this result with CRISPRi [20]. Additional genes that may be more essential in the absence of EF-P included genes encoding proline and glycine tRNAs, which decode codons at which ribosomes are more prone to stall in the absence of EF-P (Table 1). Our Tn-seq screen also identified *yebC2* (*yeel*) as a gene that may be important for growth in the absence of *efp*. *yebC2* exhibited 4-fold fewer insertions in  $\Delta efp$  compared to wild type (Table 1). To test whether YebC2 is more essential in the  $\Delta efp$  background we deleted *yebC2* from  $\Delta efp$  cells. Growth of this strain is severely impaired compared to  $\Delta efp$  or  $\Delta yebC2$  single deletions (Fig. 1A). We complemented this growth defect by providing a single copy of *yebC2* integrated into the chromosome under the control of an IPTG-inducible promoter (Fig. 1A). Moreover,  $\Delta efp\Delta yebC2$  cells also exhibit a severe decrease in polysomes consistent with a defect in protein synthesis (Fig. 1B).

Table 1

Selected genes identified as interacting with EF-P by Tn-seq

Avg. insertions in each background

<u>Gene</u>	<u>Wild type</u>	<u><math>\Delta efp</math></u>	<u>Log<sub>2</sub>(fold change)</u>
<i>yfmR</i>	147	12	- 3.6
<i>trnJ-Pro</i>	50	7	- 2.8
<i>trnI-Pro</i>	44	7	- 2.6
<i>yebC2</i> ( <i>yeel</i> )	796	192	- 2.1



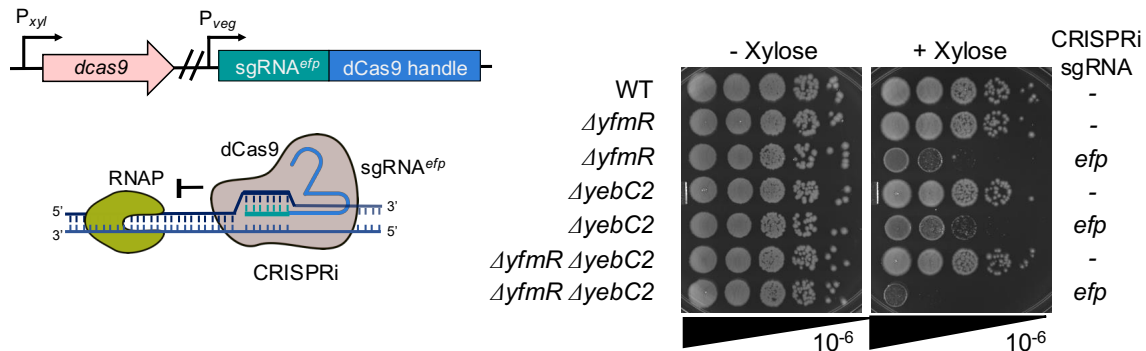
**Figure 1. Loss of *efp* and *yebC2* results in severe growth and fitness defects.**

**(A)** Growth rates of  $\Delta efp$  and  $\Delta efp\Delta yebC2$  grown in LB at 37°C. The growth defect is complemented by expressing YebC2 from a *hyperspank* promoter ( $\Delta efp\Delta yebC2 + yebC2$ ). Error bars represent standard deviation of three independent experiments and p-values represent results of an unpaired t-test with Welch's correction. **(B)** Polysome profiles of wild-type,  $\Delta efp$ , and  $\Delta efp\Delta yebC2$  strains. Representative of three independent experiments is shown. Quantification shows relative abundance of each ribosomal species as determined by area under each curve. Error bars represent standard deviation of three independent experiments.

### YebC2 is important for cellular fitness in the absence of EF-P and YfmR

We next tested whether EF-P depletion from  $\Delta yfmR\Delta yebC2$  cells would cause a more severe fitness defect than depletion of EF-P from  $\Delta yfmR$  or from  $\Delta yebC2$  single deletions using CRISPR interference [39]. We constructed a strain expressing a guide RNA (sgRNA<sup>*efp*</sup>) that blocks transcription of *efp* when expressed alongside a deactivated Cas9 (dCas9) [39,40]. We then prepared dilutions of these cells and plated them with and without xylose to induce dCas9 (Fig. 2A). Consistent with our previous observations, depleting *efp* from  $\Delta yfmR$  cells decreased colony formation by 3 orders of magnitude compared to when dCas9 was not induced. When *efp* was depleted from  $\Delta yfmR\Delta yebC2$  cells, colony formation decreased by 4 orders of magnitude (Fig. 2A). We did not detect any difference in growth or survival of  $\Delta yfmR\Delta yebC2$  double deletion. These results suggest that YebC2 is important in the  $\Delta efp$  background, and even more important in a strain lacking both EF-P and YfmR.

**A**



**B**

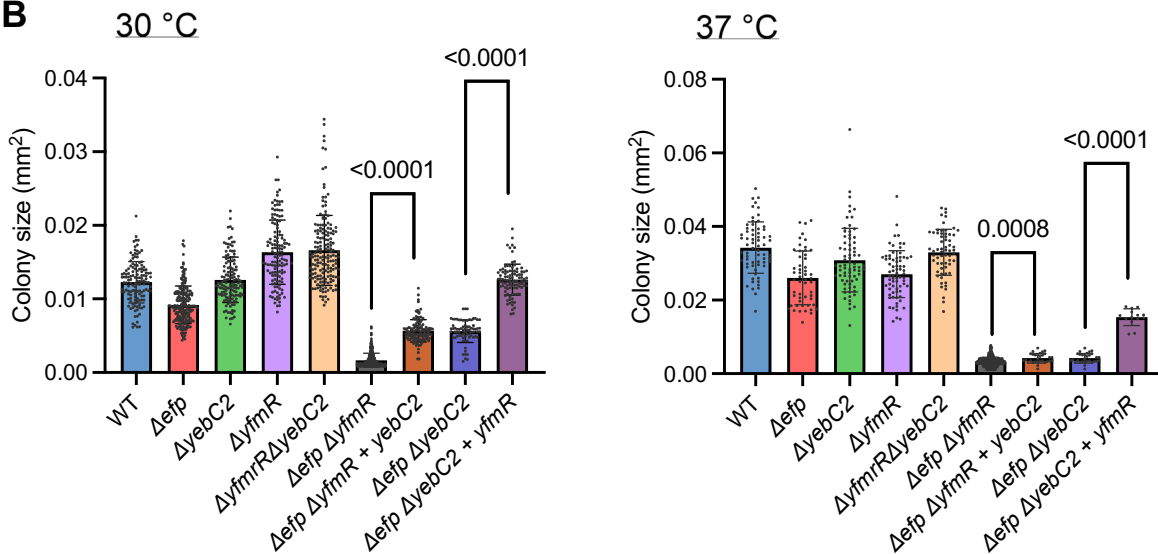


**Figure 2. Ectopic expression of YebC2 significantly increases fitness of  $\Delta efp \Delta yfmR$  cells.** (A) CRISPR interference was used to deplete EF-P from  $\Delta yfmR$ ,  $\Delta yebC2$ , or  $\Delta yfmR \Delta yebC2$  double deletion. Culture was serially diluted and plated on LB with and without xylose to induce expression of dCas9. (B) Colony area measurements indicate that expression of YebC2 in  $\Delta efp \Delta yfmR$  or expression of YfmR in  $\Delta efp \Delta yebC2$  cells partially rescues growth. LB plates were incubated at either at 30°C or 37°C. Area of resulting colonies was quantified with ImageJ. Error bars represent standard deviation and p-values represent results of an unpaired t-test with Welch's correction.

### YebC2 over-expression rescues the synthetic fitness defect of $\Delta efp \Delta yfmR$

Previously, we found that deletion of *yfmR* in *B. subtilis*  $\Delta efp::mIs$  is lethal [20]. However, removal of the erythromycin resistance marker allows construction of the  $\Delta efp \Delta yfmR$  strain, but with a severe a severe synthetic growth defect (Fig. 2B) [21]. Therefore, we tested whether over-

expression of YebC2 could rescue this synthetic defect. We expressed YebC2 under the control of an IPTG-inducible promoter in  $\Delta efp\Delta yfmR$  cells. At both 30°C and 37°C over-expression of YebC2 significantly improves fitness, as determined by colony size measurements (Fig. 2B). We next tested whether YfmR over-expression could rescue growth of  $\Delta efp\Delta yebC2$  cells. Indeed, expression of YfmR in  $\Delta efp\Delta yebC2$  cells also rescued growth as determined by colony size measurements (Fig. 2B). Since EF-P depletion from  $\Delta yfmR\Delta yebC2$  was more severe than depletion from either single mutant, and since over-expression of YebC2 or YfmR in the absence of the other two factors partially rescues growth, we conclude that YebC2, YfmR, and EF-P act independently to support growth.

### **YebC2 prevents ribosomal stalling at polyprolines**

To determine whether YebC2 is important for preventing ribosome stalling at polyprolines, we used an *in vivo* stalling reporter encoding an N-terminal Flag tag for detection and five consecutive prolines mid-way through the protein sequence (Fig. 3A). If ribosomes stall at the polyproline tract a truncated peptide is produced. Percent stalling was quantified as a percentage of stalled peptide divided by the sum of the stalled plus full-length peptide.

$\Delta yebC2$  cells exhibit ribosome stalling that is significantly higher than in wild-type cells ( $p = 0.0032$ ) (Fig. 3A). The ribosome stalling observed in  $\Delta yebC2$  cells ( $8 \pm 1\%$ ) is not as high as in  $\Delta efp$  cells ( $36 \pm 4\%$ ). However,  $\Delta efp\Delta yebC2$  exhibit very high levels of ribosome stalling ( $64 \pm 8\%$ ), significantly higher than cells deleted for just *efp* ( $p = 0.0059$ ). Moreover, YebC2 over-expression in  $\Delta efp$  cells significantly reduced ribosome stalling ( $p = 0.0062$ ). The additive increase in ribosome stalling for the  $\Delta efp\Delta yebC2$  double deletion and decreased ribosome stalling when YebC2 is over-expressed in the absence of EF-P further demonstrates that these proteins can function independently to prevent ribosome stalling. Altogether, these results demonstrate that YebC2 prevents ribosome stalling at polyproline tracts.



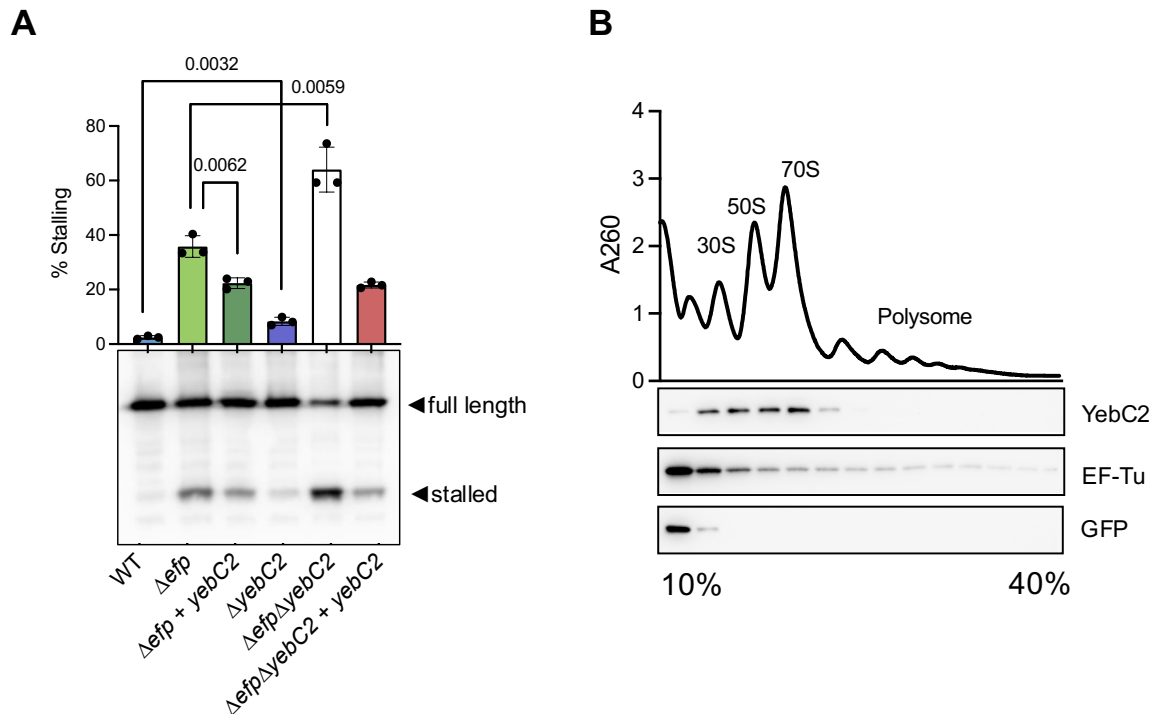


**Figure 3. YebC2 prevents ribosome stalling at a polyproline tract *in vivo* and associates with 70S ribosomes. (A)** A reporter encoding a penta-proline tract was used to monitor ribosome stalling *in vivo*. Percent stalling is reported as level of stalled protein divided by the sum of stalled and full-length protein. P-values are the result of an unpaired t-test performed on three biological replicates. Error bars indicate standard deviation. **(B)** Lysate from a strain expressing His-tagged YebC2 was resolved by sucrose density gradient ultracentrifugation. Fractions were probed with anti-His antibody or a polyclonal antibody raised against EF-Tu. His-tagged GFP was used as a negative control for ribosome association.

### YebC2 associates with 70S ribosomes

To determine whether YebC2 directly acts on the ribosome, we constructed a His-tagged version of YebC2 to monitor ribosome association. His-tagged YebC2 was functional, as evidenced by its ability to complement the impaired growth of  $\Delta efp \Delta yebC2$  cells (Fig S1). Cells expressing His-tagged YebC2 were harvested in late exponential phase, lysed, and cleared lysate was resolved on by sucrose density gradient ultracentrifugation. We found that YebC2 co-migrates with ribosomes and was strongly associated with 70S ribosomes (Fig. 3B). In contrast, a His-tagged GFP that served as a negative control for ribosome association was found only at the top of the gradient. These results suggest that YebC2 exerts its anti-stalling activity by acting directly on the ribosome.

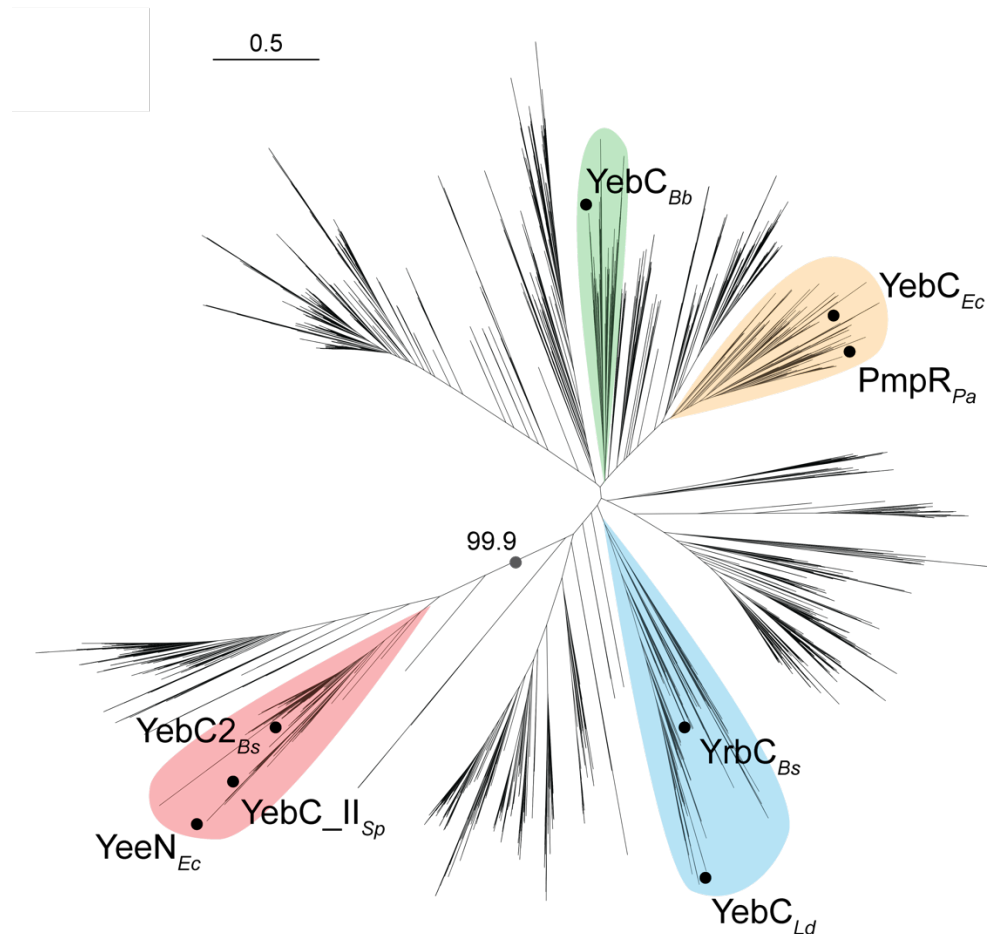


**Figure 4. YebC transcription factors are evolutionarily distinct from YebC2 translation factors.** The unrooted maximum-likelihood tree was built using all YebC family protein sequences detected in a database of >15,000 prokaryotic representative genomes. Characterized YebC family proteins are denoted with a circle and labeled with their given gene name and respective organism: *Bs*, *Bacillus subtilis*; *Ld* *Lactobacillus delbrueckii*; *Pa*, *Pseudomonas aeruginosa*; *Ec*, *Escherichia coli*; *Bb*, *Borrelia burgdorferi*; *Sp*, *Streptococcus pyogenes*. Clades containing characterized proteins were highlighted.

### YebC2 is evolutionarily distinct from YebC transcription factors

Many bacterial species encode two YebC paralogs [41]. Since most YebC paralogs studied to date are characterized transcription factors, we asked whether YebC2 clades separately from these factors. To determine the evolutionary relationship between the YebC paralogs we built a maximum likelihood tree based on the protein sequences of >15,000 YebC family proteins (Fig. 4). We found that the YebC paralogs that have experimental support for a role in transcription

(YebC from *E. coli*, *L. delbrueckii*, *B. burgdorferi* and PmpR from *P. aeruginosa*) cluster together, while those that have a role in translation (*B. subtilis* and *S. pyogenes* YebC2 and *E. coli* YeeN) cluster separately (99.9% maximum likelihood bootstrap value) (Fig. 4). YebC2 from *B. subtilis* and *S. pyogenes* share a common ancestor exclusive of the YebC proteins that have been characterized as transcription factors (100% maximum likelihood bootstrap value) (Fig. S2). Importantly, this clustering is not based on species phylogeny, since *B. subtilis* YrbC clusters with the transcription factors. Consistent with this clustering, our Tn-seq screen did not identify a genetic interaction between *yrbC* and *efp* [20]. These data suggest that YebC-family proteins have evolved separately to function in transcription or translation.

### **YebC proteins are widely distributed in bacteria while YebC2 proteins are more restricted**

Having determined that YebC and YebC2 proteins are evolutionarily distinct, we next determined the conservation of these proteins across the bacterial domain (Fig. 5). 87% of the >15,000 bacterial genomes we surveyed encode at least one YebC-family protein, consistent with a previous report of the conservation of this protein family [41]. However, YebC is much more widely distributed and highly conserved than YebC2. We detected YebC in 80% of our surveyed genomes and YebC2 in only 13%. YebC2 was mainly restricted to Firmicutes (Bacillota) and Gamma-proteobacteria. Interestingly, we found that some genomes encode up to 3 YebC paralogs and up to 2 YebC2 paralogs (Fig. 5). Further work is needed to determine whether YebC2 it is advantageous to have more than one copy of YebC2 or whether each of the YebC2 proteins has any specialized function in rescuing stalled ribosomes.

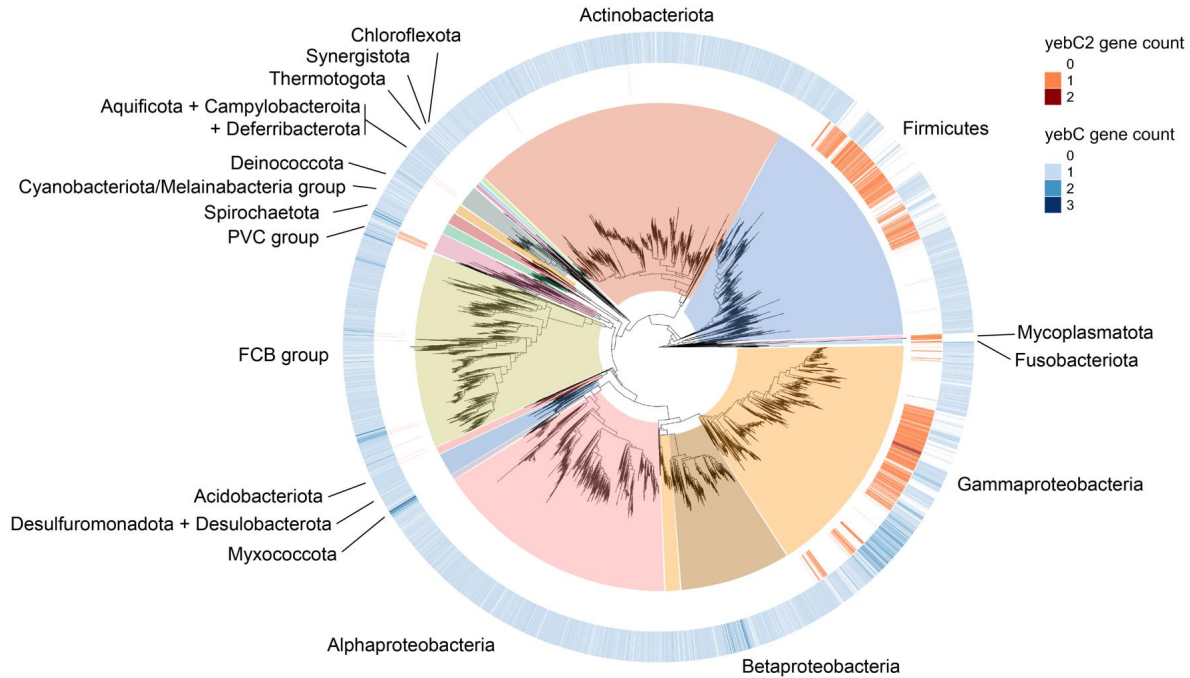


**Figure 5. Distribution of YebC-family paralogs in bacteria.** A midpoint rooted 16S maximum-likelihood phylogenetic tree of species in the bacterial domain, indicating the number of YebC2 or YebC paralogs in each genome. YebC2 paralogs are most well-conserved in Firmicutes (Bacillota), and Gamma-proteobacteria whereas YebC paralogs are widely distributed across most bacterial phyla. 87% of surveyed genomes encoded at least on YebC-family protein.

## Discussion

Here we show that YebC2 is a ribosome-binding protein that resolves ribosome stalling at a penta-proline tract *in vivo* (Fig. 3). These findings are in complete agreement with the elegant work of Brischiaglio and colleagues and Ignatov and colleagues which have likewise determined a role for human TACO1 and *S. pyogenes* YebC\_II in preventing ribosome stalling at polyprolines [37,38]. Moreover, we show that simultaneous loss of YebC2, EF-P, and YfmR severely reduces the viability of *B. subtilis*, and present evidence that YebC2 prevents ribosome stalling independent of EF-P and YfmR (Fig. 2). These data contribute to a more complete understanding of the various factors that prevent ribosome stalling at polyproline tracts.

YebC family proteins have been widely annotated as transcription factors [31–34,42,43]. By analyzing YebC and YebC2 protein sequences, we found that these proteins cluster into divergent clades in good agreement with experimental evidence supporting their roles in either transcription or translation (Fig. 4). In particular, *B. subtilis* and *S. pyogenes* YebC2 share a common ancestor that is exclusive of the YebC transcription factors. However, it is notable that *E. coli* YebC resolves ribosome stalling at a penta-proline tract despite its role in transcription [34] and the fact that it clusters with the YebC transcription factors (Fig. 4). Do YebC transcription factors also play a role in translation? While it is clear that YebC and YebC2 are evolutionarily distinct, more work is needed to fully characterize their functional divergence.

We also determined the conservation of YebC and YebC2 paralogs across the bacterial domain. YebC2 is conserved primarily within Firmicutes (Bacillota) and Gamma-proteobacteria (Fig. 5). YebC is more broadly distributed, with homologs detected in most phyla. The retention of both YebC and YebC2 paralogs in many taxa further supports a model in which these proteins impart unique selective advantages due to independent functions. It is notable that although the transcription-family YebC proteins are broadly distributed in bacteria, eukaryotes encode only the YebC2-type protein [41].

Our data support a model in which EF-P, YfmR, and YebC2 can each function independently to prevent ribosome stalling. An independent role for YebC2 is demonstrated by its ability to prevent stalling on an *in vivo* reporter in  $\Delta yfmR\Delta efp$  cells and its ability to partially complement the severe synthetic growth defect of  $\Delta yfmR\Delta efp$  cells (Fig. 2). If YebC2 were absolutely dependent on either EF-P or YfmR for its activity, it would be unable to rescue growth or prevent ribosome stalling in the  $\Delta efp\Delta yfmR$  background. Interestingly, while EF-P and YfmR have partially overlapping binding sites in the ribosomal E-site, some evidence suggests that YebC2 may bind the A-site. First, proximity labeling with a TACO1-BirA fusion protein resulted in biotin labeling of A-site adjacent ribosomal proteins [37]. Second, sequencing of RNA cross-linked to YebC\_II in *S. pyogenes* revealed likely contacts with Helix 89 [38]. If YebC2 and its homologs can bind the ribosomal A-site while EF-P or YfmR are bound in the E-site, then it remains an exciting possibility that there are some forms of ribosome stalling where YebC2 does indeed aid the activity of either EF-P or YfmR.

Although we observe anti-stalling activity for EF-P, YfmR, and YebC2 on a penta-proline reporter, it is likely that all of these factors prevent ribosome stalling at sequences that extend beyond prolines. For example, YfmR also prevents ribosome stalling on polyacidic residues [21]. Meanwhile, EF-P promotes peptide bond formation at other difficult-to-translate sequences [44,45]. In particular, EF-P likely plays a role in formation of the first peptide bond since it recognizes both tRNA<sup>Pro</sup> and initiating tRNA<sup>Met</sup> in the P-site [11,46]. Moreover, EF-P promotes peptide bond formation between initiating formyl-methionine and the second amino acid and helps maintain the reading frame during early elongation [47–49]. There is some evidence that YfmR may also participate in early elongation since YfmR depletion in  $\Delta efp$  cells causes increased association of initiator tRNA with stalled ribosomes [20]. There is also evidence that YebC2 plays a role at non-proline encoding sequences since deletion of the YebC2 ortholog in yeast causes a more general defect in protein synthesis, with reduced overall synthesis of mitochondrial-localized reporters [50].

Although structurally distinct, both EF-P and YfmR make similar contacts with the P-site tRNA, and both exhibit tRNA mimicry, which is common for ribosome-binding proteins [51]. The YebC2 predicted structure does not align well with either EF-P or YfmR and so its mechanism of action is likely to be completely different, especially if it binds the ribosomal A-site. Nevertheless, proximity labeling with TACO1 and RNA crosslinking with YebC\_II indicate that these proteins likely contact the peptidyl-transferase center, and may therefore directly stimulate peptide bond formation [37,38]. Structural studies of YfmR on a polyproline substrate, and of YebR bound the ribosome are essential to our understanding of how these proteins resolve ribosome stalling.

## Materials and Methods

### Strains and media

Strains were derived from *B. subtilis* 168 trpC2 and are listed in Table 1. Single deletions were obtained from the BKK collection [52] and moved into the lab's 168 trpC2 strain by natural transformation. The kanamycin resistance cassette was excised to make clean deletions using pDR244 [52]. *B. subtilis* strains were cultured in LB and supplemented with antibiotics at final concentrations of 100 µg/mL spectinomycin, 1x MLS (1 µg/mL erythromycin and 25 µg/mL lincomycin), or 5 µg/mL chloramphenicol. *E. coli* DH5alpha strains were cultured in LB with 100 µg/mL ampicillin.

### Complementation of *yebC2* and *yfmR*

Primers are listed in Table 1. *yeeI* was amplified from the wild-type *B. subtilis* 1772 WT 168 trpC2 genomic DNA using primers HRH155 and HRH156 which contain 22 bp of homology to pDR111. Primers HRH157 and HRH158 were used to amplify *yfmR*. The resulting fragments were cloned by Gibson assembly into pDR111 cut with HindIII and SphI. The resulting plasmids, pHRH703 ( $P_{hyper-yeeI}$ ) and pHRH706 ( $P_{hyper-YfmR}$ ) were linearized with Scal and transformed for integration on the chromosome at *amyE*.

### Growth Curves

*B. subtilis* strains were grown overnight at room temperature, and inoculated to a final OD<sub>600</sub> 0.05 in 150 µl LB, and supplemented with 1 mM IPTG where appropriate in a 96 well-plate (ThermoScientific 167008). The cultures were incubated at 30 °C and 37 °C with linear shaking (2-mm intensity). OD<sub>600</sub> of strains were measured at 15-min intervals over 20 hours using a microplate reader (BioTek).



## Colony Size Measurement

*B. subtilis* strains were cultured in LB at room temperature or 37 °C overnight in a roller drum at 80 rpm. 1 mM IPTG was added to the strains overexpressing Yeel or YfmR. The cells were normalized to OD<sub>600</sub> 0.05 and serially diluted and plated onto two LB agar plates. These plates were incubated at 30 °C or 37 °C for 24 hours, and then placed at room temperature for 24 hours. The plates were imaged on ChemiDoc<sup>TM</sup>MP (Biorad), and the area of the individual colonies was measured using ImageJ [53].

## CRISPRi Depletion

Primer HRH sgRNA-efp-3 containing an sgRNA sequence (5'-tcgcgccagtgccaaggttg-3') was designed to target EF-P. HRH sgRNA-efp-3 and HRH175 [20] were used to amplify pJMP2 [40], generating pHRH1021. pJMP1 carrying dCas9 under the xylose-inducible promoter [40] was transformed into the single deletion strains  $\Delta yeel::kan$  (HAF450) and  $\Delta yfmR::kan$  (HAF451) and the double deletion strain  $\Delta yeel\Delta yfmR$  (HRH1132). Next, pHRH1021 was transformed into the strains harboring dCas9, therefore producing EF-P depletion strains. The resulting *B. subtilis* CRISPRi knockdown strains were cultured overnight without xylose and diluted to an OD<sub>600</sub> of 0.05 in LB. The cultures were subsequently diluted 10-fold as 10<sup>-2</sup> to 10<sup>-6</sup> and spotted onto LB agar without xylose or onto LB agar containing 5% xylose.

## Proline Stalling Reporter and Western Blot

The RFP-CFP fusion cassette containing the pentaproline stalling motifs (5'-ccaccaccaccacc-3') or the reporter cassette without the motifs were amplified by using primers HRH204 and HRH205 from the previous constructs pHRH899 and pHRH903 (Table 1). The resulting fragments were cloned into the empty pECE174 [54] plasmid cut with EcoRI and BamHI, producing pHRH1169 and pHRH1173. The resulting reporter plasmids were sequenced by Plasmidsaurus and linearized with Scal to transform into the different combinations of deletions in *B. subtilis* for

recombination at *sacA*. The reporter strains were grown overnight and then diluted back to OD<sub>600</sub> 0.05. The diluted cultures were induced with 1 mM IPTG and grown up to OD<sub>600</sub> 1.2 at 37 °C in a roller drum at 90 rpm. 1-mL cell cultures were collected and resuspended with 60 µL of lysis buffer (10 mM Tris pH 8, 50 mM EDTA, 1 mg/mL lysozyme), then incubated at 37 °C for 10 min. Next, the cell lysates were resuspended with 40 µL 4x SDS-PAGE loading buffer. The lysate samples were heated at 85 °C for 5 min and immediately cooled on ice. 10 µL samples were loaded onto a 12 % SDS-PAGE gel and run at 150 V for 70 min. The protein was transferred to PVDF membrane (Biorad) at 300 mA for 100 min. The membrane was blocked with 3 % BSA for 20 min and incubated with 4 µg anti-FLAG monoclonal antibody (Sigma SAB4200119) for 20 min at room temperature. The membrane was washed 3 times with PBS-T and developed with ECL (Biorad170-5060) for 2 min and imaged on ChemiDoc<sup>TM</sup>MP (Biorad).

### **Polysome Profiling**

Strains were grown overnight at 37 °C and inoculated to an OD<sub>600</sub> of 0.05 in 40 ml LB the next morning. Cells were collected at OD<sub>600</sub> 1.2 by centrifugation at 8000 rpm for 10 minutes (Beckman Coulter Avanti J-15R, rotor JA-10.100). Cell pellets were resuspended in 200 µl gradient buffer containing 20 mM Tris (pH 7.4 at 4°C), 0.5 mM EDTA, 60 mM NH<sub>4</sub>Cl, and 7.5 mM MgCl<sub>2</sub> and 6mM 2-mercaptoethanol. Cells lysed using a homogenizer (Beadbug6, Benchmark) by five 20 second pulses at speed 4350 rpm with chilling on ice for 2 min between the cycles and clarified by centrifugation at 21,300 rcf for 20 min (Eppendorf 5425R, rotor FA-24x2). Clarified lysates were normalized to 1500 ng/µl and loaded onto 10 – 40% sucrose gradients in gradient buffer and run for 3 hours at 30,000 rpm at 4°C in an SW-41Ti rotor. Gradients were collected using a Biocomp Gradient Station (BioComp Instruments) with A260 continuous readings (Triax full spectrum flow cell). The area under each peak was quantified using Graphpad Prism.

### **Gene detection**

Genes were detected in a database of >18,000 representative prokaryotic genomes from NCBI RefSeq using HMMER v3.3 (nhmmer) (hmmmer.org) with an E-value cutoff of 0.05 and a query of all characterized *yebC*-family gene sequences. Hits were classified as either *yebC* or *yebC2* depending on the gene query that resulted in a higher sequence bit score, and therefore greater homology. Genomes were filtered for <10% CheckM contamination [55], which left us with 15,259 genomes to survey.

### **Phylogenetics**

16S rRNA sequences of all genomes were identified and acquired using BLAST v2.13.0, aligned using MAFFT v7.453, and applied to FastTree v2.1.11 [56] to infer a maximum likelihood tree [57]. FastTree produces unrooted phylogenies, so the tree was midpoint rooted using the phangorn v2.11.1 package [58]. Taxonomic classification was assigned to genomes using the NCBI Taxonomy database [59] and taxonkit v0.17.0 [60]. Phyla were named using the conventions in Coleman et al. 2021 [61]. The tree was visualized using ggtree v3.12.0 [62]. For the large YebC-family tree, the gene sequences of HMMER hits were translated using a Python script, and the tree was built and visualized using the same pipeline as described previously.

### **Acknowledgements**

H-RH, CRP, and HAF were supported by NIH R35GM147049. CRP was supported by a Graduate Research Fellowship from the National Science Foundation. We are grateful to Tory Hendry, Vasili Hauryliuk, Katrina Callan, Kevin England, and Daniel Tetreault for feedback on the manuscript.

1 Table 2

2	<b><u>Strain (strain number)</u></b>	<b><u>Description</u></b>	<b><u>Source</u></b>
3	HAF1	168 trpC2 <i>B. subtilis</i> wild type	[63]
4	HAF242	168 trpC2 $\Delta$ efp:: <i>kan</i>	[19]
5	HAF450	168 trpC2 $\Delta$ yeel:: <i>kan</i>	This study
6	HAF451	168 trpC2 $\Delta$ yfmR:: <i>kan</i>	This study
7	HRH575	168 trpC2 $\Delta$ efp	This study
8	HRH802	168 trpC2 $\Delta$ yeel	This study
9	HRH804	168 trpC2 $\Delta$ yfmR	This study
10	HAF519	168 trpC2 $\Delta$ efp $\Delta$ yeel:: <i>kan</i>	This study
11	HAF521	168 trpC2 $\Delta$ efp $\Delta$ yfmR:: <i>kan</i>	This study
12	HRH1132	168 trpC2 $\Delta$ yeel:: <i>kan</i> $\Delta$ yfmR	This study
13	HAF518	168 trpC2 $\Delta$ efp $\Delta$ yeel:: <i>kan</i> amyE:: <i>P<sub>hyper</sub>-YfmR</i>	This study
14	HAF527	168 trpC2 $\Delta$ efp $\Delta$ yeel:: <i>kan</i> amyE:: <i>P<sub>hyper</sub>-Yeel</i>	This study
15	HAF528	168 trpC2 $\Delta$ efp $\Delta$ yfmR amyE:: <i>P<sub>hyper</sub>-Yeel</i>	This study
16	HRH774	168 trpC2 WT lacA:: <i>P<sub>xyI</sub>-dCas9</i>	This study
17	HRH776	168 trpC2 $\Delta$ efp:: <i>kan</i> lacA:: <i>P<sub>xyI</sub>-dCas9</i>	This study
18	HRH1022	168 trpC2 $\Delta$ yfmR:: <i>kan</i> lacA:: <i>P<sub>xyI</sub>-dCas9</i>	This study
19	HRH1024	168 trpC2 $\Delta$ yeel:: <i>kan</i> lacA:: <i>P<sub>xyI</sub>-dCas9</i>	This study
20	HRH1134	168 trpC2 $\Delta$ yeel:: <i>kan</i> $\Delta$ yfmR lacA:: <i>P<sub>xyI</sub>-dCas9</i>	This study

21	HRH829	168 trpC2 $\Delta$ efp:: <i>kan lacA</i> ::P <sub>xyl</sub> -dCas9 <i>amyE</i> ::P <sub>veg</sub> -sgRNA <sup>yeel</sup>	This study
22	HRH1042	168 trpC2 $\Delta$ yfmR:: <i>kan lacA</i> ::P <sub>xyl</sub> -dCas9 <i>amyE</i> ::P <sub>veg</sub> -sgRNA <sup>efp</sup>	This study
23	HRH1053	168 trpC2 $\Delta$ yeel:: <i>kan lacA</i> ::P <sub>xyl</sub> -dCas9 <i>amyE</i> ::P <sub>veg</sub> -sgRNA <sup>efp</sup>	This study
24	HRH1137	168 trpC2 $\Delta$ yeel:: <i>kan <math>\Delta</math>yfmR lacA</i> ::P <sub>xyl</sub> -dCas9 <i>amyE</i> ::P <sub>veg</sub> -sgRNA <sup>efp</sup>	This study
25	HRH1177	168 trpC2 WT <i>sacA</i> ::P <sub>hyper</sub> -3xFLAG- <i>rfp-cfp</i>	This study
26	HRH1193	168 trpC2 $\Delta$ efp <i>sacA</i> ::P <sub>hyper</sub> -3xFLAG- <i>rfp-cfp</i>	This study
27	HRH1178	168 trpC2 $\Delta$ yfmR <i>sacA</i> ::P <sub>hyper</sub> -3xFLAG- <i>rfp-cfp</i>	This study
28	HRH1179	168 trpC2 $\Delta$ yeel <i>sacA</i> ::P <sub>hyper</sub> -3xFLAG- <i>rfp-cfp</i>	This study
29	HRH1195	168 trpC2 $\Delta$ efp $\Delta$ yfmR:: <i>kan sacA</i> ::P <sub>hyper</sub> -3xFLAG- <i>rfp-cfp</i>	This study
30	HRH1197	168 trpC2 $\Delta$ efp $\Delta$ yeel <i>sacA</i> ::P <sub>hyper</sub> -3xFLAG- <i>rfp-cfp</i>	This study
31	HRH1180	168 trpC2 $\Delta$ yeel $\Delta$ yfmR <i>sacA</i> ::P <sub>hyper</sub> -3xFLAG- <i>rfp-cfp</i>	This study
32	HRH1185	168 trpC2 $\Delta$ efp <i>amyE</i> ::P <sub>hyper</sub> -YfmR <i>sacA</i> ::P <sub>hyper</sub> -3xFLAG- <i>rfp-cfp</i>	This study
33	HRH1187	168 trpC2 $\Delta$ efp <i>amyE</i> ::P <sub>hyper</sub> -Yeel <i>sacA</i> ::P <sub>hyper</sub> -3xFLAG- <i>rfp-cfp</i>	This study
34	HRH1199	168 trpC2 $\Delta$ efp $\Delta$ yfmR:: <i>kan amyE</i> ::P <sub>hyper</sub> -Yeel <i>sacA</i> ::P <sub>hyper</sub> -3xFLAG- <i>rfp-cfp</i>	This study
35	HRH1201	168 trpC2 $\Delta$ efp $\Delta$ yeel:: <i>kan amyE</i> ::P <sub>hyper</sub> -YfmR <i>sacA</i> ::P <sub>hyper</sub> -3xFLAG- <i>rfp-cfp</i>	This study
36	HRH1203	168 trpC2 $\Delta$ efp $\Delta$ yeel:: <i>kan amyE</i> ::P <sub>hyper</sub> -Yeel <i>sacA</i> ::P <sub>hyper</sub> -3xFLAG- <i>rfp-cfp</i>	This study
37	HRH1205	168 trpC2 $\Delta$ efp $\Delta$ yfmR:: <i>kan amyE</i> ::P <sub>hyper</sub> -YfmR <i>sacA</i> ::P <sub>hyper</sub> -3xFLAG- <i>rfp-cfp</i>	This study
38	HRH1181	168 trpC2 WT <i>sacA</i> ::P <sub>hyper</sub> -3xFLAG- <i>rfp-5xprolines-cfp</i>	This study
39	HRH1194	168 trpC2 $\Delta$ efp <i>sacA</i> ::P <sub>hyper</sub> -3xFLAG- <i>rfp-5xprolines-cfp</i>	This study
40	HRH1182	168 trpC2 $\Delta$ yfmR <i>sacA</i> ::P <sub>hyper</sub> -3xFLAG- <i>rfp-5xprolines-cfp</i>	This study

41	HRH1183	168 trpC2 $\Delta$ yeel sacA::P <sub>hyper</sub> -3xFLAG-rfp-5xprolines-cfp	This study
42	HRH1207	168 trpC2 $\Delta$ efp $\Delta$ yfmR::kan sacA::P <sub>hyper</sub> -3xFLAG-rfp-5xprolines-cfp	This study
43	HRH1209	168 trpC2 $\Delta$ efp $\Delta$ yeel::kan sacA::P <sub>hyper</sub> -3xFLAG-rfp-5xprolines-cfp	This study
44	HRH1184	168 trpC2 $\Delta$ yeel $\Delta$ yfmR sacA::P <sub>hyper</sub> -3xFLAG-rfp-5xprolines-cfp	This study
45	HRH1190	168 trpC2 $\Delta$ efp amyE::P <sub>hyper</sub> -YfmR sacA::P <sub>hyper</sub> -3xFLAG-rfp-5xprolines-cfp	This study
46	HRH1191	168 trpC2 $\Delta$ efp amyE::P <sub>hyper</sub> -Yeel sacA::P <sub>hyper</sub> -3xFLAG-rfp-5xprolines-cfp	This study
47	HRH1211	168 trpC2 $\Delta$ efp $\Delta$ yfmR::kan amyE::P <sub>hyper</sub> -Yeel sacA::P <sub>hyper</sub> -3xFLAG-rfp-5xprolines-cfp	This study
48	HRH1213	168 trpC2 $\Delta$ efp $\Delta$ yeel::kan amyE::P <sub>hyper</sub> -YfmR sacA::P <sub>hyper</sub> -3xFLAG-rfp-5xprolines-cfp	This study
49	HRH1215	168 trpC2 $\Delta$ efp $\Delta$ yeel::kan amyE::P <sub>hyper</sub> -Yeel sacA::P <sub>hyper</sub> -3xFLAG-rfp-5xprolines-cfp	This study
50	HRH1217	168 trpC2 $\Delta$ efp $\Delta$ yfmR::kan amyE::P <sub>hyper</sub> -YfmR sacA::P <sub>hyper</sub> -3xFLAG-rfp-5xprolines-cfp	This study
51	<b><u>Plasmid</u></b>	<b><u>Description</u></b>	<b><u>Source</u></b>
52	pHRH703	pDR111 amyE::P <sub>hyper</sub> - <i>B. subtilis</i> Yeel	This study
53	pHRH706	pDR111 amyE::P <sub>hyper</sub> - <i>B. subtilis</i> YfmR	[20]
54	pHRH1021	pJMP2 amyE::P <sub>veg</sub> -sgRNA <sup>efp</sup>	This study
55	pHRH819	pJMP2 amyE::P <sub>veg</sub> -sgRNA <sup>yeel</sup>	This study
56	pHRH899	pDR111 amyE::P <sub>hyper</sub> -3xFLAG-rfp-cfp	[20]
57	pHRH903	pDR111 amyE::P <sub>hyper</sub> -3xFLAG-rfp-5xprolines-cfp	[20]
58	pECE174	SacA integration plasmid to <i>B. subtilis</i>	[54]
59	pHRH1169	pECE174 sacA::P <sub>hyper</sub> -3xFLAG-rfp-cfp	This study
60	pHRH1173	pECE174 sacA::P <sub>hyper</sub> -3xFLAG-rfp-5xprolines-cfp	This study

61	<b><u>Primer</u></b>	<b><u>Sequence</u></b>	<b><u>Source</u></b>
62	HRH sgRNA-efp-3	5'- gctcgtgtgtacaataaatgtatcgcgccagtgccaaggttggttttagagctagaaatagcaagttaaataaggc -3'	This study
63	HRH sgRNA-Yeel-3	5'- gctcgtgtgtacaataaatgtacgccgccacataaatctcagtttttagagctagaaatagcaagttaaataaggc -3'	This study
64	HRH175	5'- acatttattgtacaacacgagcc-3'	[20]
65	HRH155	5'- taattgtgagcggataacaattaagcttgaggaaaaaaaaatgggccgtaagtggaaca -3'	This study
66	HRH156	5'- ctcgttccaccgaattagcttgcattactcacctaaatcaacgttatgatatacc -3'	This study
67	HRH157	5'- attgtgagcggataacaattaagcttgaggaaaaaaaaatgagcatattaaagcggaa -3'	This study
68	HRH158	5'- acctcgttccaccgaattagcttgcatttagctttccagttctcga -3'	This study
69	HRH204	5'- gccgatgataagctgtcaaacatgagaattcgactctctagcttgaggcatc -3'	This study
70	HRH205	5'- tggtaatggtagcgcaccggcgctcaggatcctaactcacattaattgcgttgc -3'	This study

71 **REFERENCES**

- 72
- 73 1. Doerfel LK, Wohlgemuth I, Kubyshev V, Starosta AL, Wilson DN, Budisa N, et al. Entropic  
74 Contribution of Elongation Factor P to Proline Positioning at the Catalytic Center of the  
75 Ribosome. *J Am Chem Soc.* 2015;137: 12997–13006. doi:10.1021/jacs.5b07427
- 76 2. Huter P, Arenz S, Bock LV, Graf M, Frister JO, Heuer A, et al. Structural Basis for  
77 Polyproline-Mediated Ribosome Stalling and Rescue by the Translation Elongation Factor EF-P.  
78 *Mol Cell.* 2017;68: 515-527.e6. doi:10.1016/j.molcel.2017.10.014
- 79 3. Glick BR, Ganoza MC. Identification of a soluble protein that stimulates peptide bond  
80 synthesis. *Proc Natl Acad Sci U S A.* 1975;72: 4257–60. doi:10.1073/pnas.72.11.4257
- 81 4. Ude S, Lassak J, Starosta AL, Kraxenberger T, Wilson DN, Jung K. Translation elongation  
82 factor EF-P alleviates ribosome stalling at polyproline stretches. *Science.* 2013;339: 82–5.  
83 doi:10.1126/science.1228985
- 84 5. Doerfel LK, Wohlgemuth I, Kothe C, Peske F, Urlaub H, Rodnina MV. EF-P is essential for  
85 rapid synthesis of proteins containing consecutive proline residues. *Science.* 2013;339: 85–8.  
86 doi:10.1126/science.1229017
- 87 6. Woolstenhulme CJ, Parajuli S, Healey DW, Valverde DP, Petersen EN, Starosta AL, et al.  
88 Nascent peptides that block protein synthesis in bacteria. *Proc Natl Acad Sci U S A.* 2013;110:  
89 E878-887. doi:10.1073/pnas.1219536110
- 90 7. Peil L, Starosta AL, Lassak J, Atkinson GC, Virumäe K, Spitzer M, et al. Distinct XPPX  
91 sequence motifs induce ribosome stalling, which is rescued by the translation elongation factor  
92 EF-P. *Proc Natl Acad Sci U S A.* 2013;110: 15265–15270. doi:10.1073/pnas.1310642110
- 93 8. Bullwinkle TJ, Zou SB, Rajkovic A, Hersch SJ, Elgamal S, Robinson N, et al. (R)- $\beta$ -lysine-  
94 modified elongation factor P functions in translation elongation. *J Biol Chem.* 2013;288: 4416–  
95 4423. doi:10.1074/jbc.M112.438879
- 96 9. Starosta AL, Lassak J, Peil L, Atkinson GC, Woolstenhulme CJ, Virumäe K, et al. A  
97 conserved proline triplet in Val-tRNA synthetase and the origin of elongation factor P. *Cell Rep.*  
98 2014;9: 476–483. doi:10.1016/j.celrep.2014.09.008
- 99 10. Mohapatra S, Choi H, Ge X, Sanyal S, Weisshaar JC. Spatial Distribution and Ribosome-  
100 Binding Dynamics of EF-P in Live *Escherichia coli*. *mBio.* 2017;8: e00300-17.  
101 doi:10.1128/mBio.00300-17
- 102 11. Mudryi V, Frister JO, Peng B-Z, Wohlgemuth I, Peske F, Rodnina MV. Kinetic mechanism  
103 and determinants of EF-P recruitment to translating ribosomes. *Nucleic Acids Res.* 2024;  
104 gkae815. doi:10.1093/nar/gkae815
- 105 12. DeJesus MA, Gerrick ER, Xu W, Park SW, Long JE, Boutte CC, et al. Comprehensive  
106 Essentiality Analysis of the *Mycobacterium tuberculosis* Genome via Saturating Transposon  
107 Mutagenesis. *mBio.* 2017;8: e02133-16. doi:10.1128/mBio.02133-16
- 108 13. Yanagisawa T, Takahashi H, Suzuki T, Masuda A, Dohmae N, Yokoyama S. *Neisseria*  
109 *meningitidis* Translation Elongation Factor P and Its Active-Site Arginine Residue Are Essential  
110 for Cell Viability. *PLoS One.* 2016;11: e0147907. doi:10.1371/journal.pone.0147907
- 111 14. Guo Q, Cui B, Wang M, Li X, Tan H, Song S, et al. Elongation factor P modulates  
112 *Acinetobacter baumannii* physiology and virulence as a cyclic dimeric guanosine  
113 monophosphate effector. *Proc Natl Acad Sci U S A.* 2022;119: e2209838119.  
114 doi:10.1073/pnas.2209838119



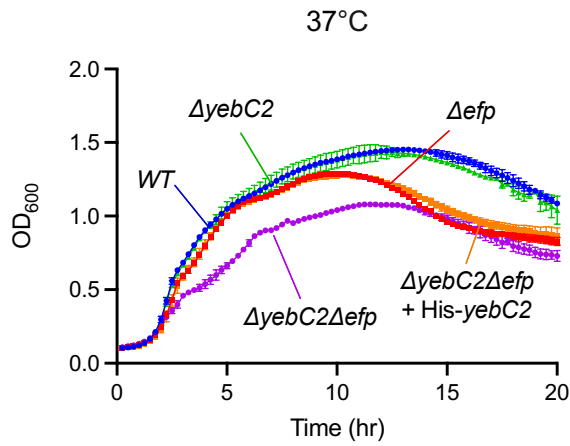
- 115 15. Kearns DB, Chu F, Rudner R, Losick R. Genes governing swarming in *Bacillus subtilis* and  
116 evidence for a phase variation mechanism controlling surface motility. *Mol Microbiol.* 2004;52:  
117 357–369. doi:10.1111/j.1365-2958.2004.03996.x
- 118 16. Rajkovic A, Hummels KR, Witzky A, Erickson S, Gafken PR, Whitelegge JP, et al.  
119 Translation Control of Swarming Proficiency in *Bacillus subtilis* by 5-Amino-pentanoylated  
120 Elongation Factor P. *J Biol Chem.* 2016;291: 10976–10985. doi:10.1074/jbc.M115.712091
- 121 17. Tollerson R, Witzky A, Ibba M. Elongation factor P is required to maintain proteome  
122 homeostasis at high growth rate. *Proc Natl Acad Sci U S A.* 2018;115: 11072–11077.  
123 doi:10.1073/pnas.1812025115
- 124 18. Hummels KR, Kearns DB. Suppressor mutations in ribosomal proteins and FliY restore  
125 *Bacillus subtilis* swarming motility in the absence of EF-P. *PLoS Genet.* 2019;15: e1008179.  
126 doi:10.1371/journal.pgen.1008179
- 127 19. Feaga HA, Hong H-R, Prince CR, Rankin A, Buskirk AR, Dworkin J. Elongation Factor P Is  
128 Important for Sporulation Initiation. *J Bacteriol.* 2023;205: e0037022. doi:10.1128/jb.00370-22
- 129 20. Hong H-R, Prince CR, Tetreault DD, Wu L, Feaga HA. YfmR is a translation factor that  
130 prevents ribosome stalling and cell death in the absence of EF-P. *Proc Natl Acad Sci U S A.*  
131 2024;121: e2314437121. doi:10.1073/pnas.2314437121
- 132 21. Takada H, Fujiwara K, Atkinson GC, Chiba S, Haurlyliuk V. Resolution of ribosomal stalling  
133 by EF-P and ABCF ATPases YfmR and YkpA/YbiT. *Nucleic Acids Res.* 2024;52: 9854–9866.  
134 doi:10.1093/nar/gkae556
- 135 22. Boël G, Smith PC, Ning W, Englander MT, Chen B, Hashem Y, et al. The ABC-F protein  
136 EttA gates ribosome entry into the translation elongation cycle. *Nat Struct Mol Biol.* 2014;21:  
137 143–151. doi:10.1038/nsmb.2740
- 138 23. Murina V, Kasari M, Takada H, Hinnu M, Saha CK, Grimshaw JW, et al. ABCF ATPases  
139 Involved in Protein Synthesis, Ribosome Assembly and Antibiotic Resistance: Structural and  
140 Functional Diversification across the Tree of Life. *J Mol Biol.* 2019;431: 3568–3590.  
141 doi:10.1016/j.jmb.2018.12.013
- 142 24. Ousalem F, Ngo S, Oïffer T, Omairi-Nasser A, Hamon M, Monlezun L, et al. Global  
143 regulation via modulation of ribosome pausing by the ABC-F protein EttA. *Nat Commun.*  
144 2024;15: 6314. doi:10.1038/s41467-024-50627-z
- 145 25. Kerr ID, Reynolds ED, Cove JH. ABC proteins and antibiotic drug resistance: is it all about  
146 transport? *Biochem Soc Trans.* 2005;33: 1000–1002. doi:10.1042/BST20051000
- 147 26. Wilson DN. The ABC of Ribosome-Related Antibiotic Resistance. *mBio.* 2016;7: e00598-  
148 16. doi:10.1128/mBio.00598-16
- 149 27. Murina V, Kasari M, Haurlyliuk V, Atkinson GC. Antibiotic resistance ABCF proteins reset  
150 the peptidyl transferase centre of the ribosome to counter translational arrest. *Nucleic Acids*  
151 *Res.* 2018;46: 3753–3763. doi:10.1093/nar/gky050
- 152 28. Chadani Y, Yamanouchi S, Uemura E, Yamasaki K, Niwa T, Ikeda T, et al. The ABCF  
153 proteins in *Escherichia coli* individually cope with “hard-to-translate” nascent peptide  
154 sequences. *Nucleic Acids Res.* 2024;52: 5825–5840. doi:10.1093/nar/gkae309
- 155 29. Ousalem F, Singh S, Bailey NA, Wong K-H, Zhu L, Neky MJ, et al. Comparative genetic,  
156 biochemical, and biophysical analyses of the four *E. coli* ABCF paralogs support distinct  
157 functions related to mRNA translation. *bioRxiv.* 2023; 2023.06.11.543863.  
158 doi:10.1101/2023.06.11.543863

- 159 30. Shikha Singh, Riley C. Gentry, Ziao Fu, Nevette A. Bailey, Clara G. Altomare, Kam-Ho  
160 Wong, et al. Cryo-EM studies of the four E. coli paralogs establish ABCF proteins as master  
161 plumbers of the peptidyl-transferase center of the ribosome. *bioRxiv*. 2023.  
162 doi:<https://doi.org/10.1101/2023.06.15.543498>
- 163 31. Liang H, Li L, Dong Z, Surette MG, Duan K. The YebC family protein PA0964 negatively  
164 regulates the *Pseudomonas aeruginosa* quinolone signal system and pyocyanin production. *J*  
165 *Bacteriol*. 2008;190: 6217–6227. doi:10.1128/JB.00428-08
- 166 32. Brown L, Villegas JM, Elean M, Fadda S, Mozzi F, Saavedra L, et al. YebC, a putative  
167 transcriptional factor involved in the regulation of the proteolytic system of *Lactobacillus*. *Sci*  
168 *Rep*. 2017;7: 8579. doi:10.1038/s41598-017-09124-1
- 169 33. Zhang Y, Chen T, Raghunandan S, Xiang X, Yang J, Liu Q, et al. YebC regulates variable  
170 surface antigen VlsE expression and is required for host immune evasion in *Borrelia burgdorferi*.  
171 *PLoS Pathog*. 2020;16: e1008953. doi:10.1371/journal.ppat.1008953
- 172 34. Choi E, Jeon H, Oh C, Hwang J. Elucidation of a Novel Role of YebC in Surface  
173 Polysaccharides Regulation of *Escherichia coli* bipA-Deletion. *Front Microbiol*. 2020;11: 597515.  
174 doi:10.3389/fmicb.2020.597515
- 175 35. Weraarpachai W, Antonicka H, Sasarman F, Seeger J, Schrank B, Kolesar JE, et al.  
176 Mutation in TACO1, encoding a translational activator of COX I, results in cytochrome c oxidase  
177 deficiency and late-onset Leigh syndrome. *Nat Genet*. 2009;41: 833–837. doi:10.1038/ng.390
- 178 36. Richman TR, Spåhr H, Ermer JA, Davies SMK, Viola HM, Bates KA, et al. Loss of the RNA-  
179 binding protein TACO1 causes late-onset mitochondrial dysfunction in mice. *Nat Commun*.  
180 2016;7: 11884. doi:10.1038/ncomms11884
- 181 37. Brischigliaro M, Krüger A, Moran JC, Antonicka H, Ahn A, Shoubridge EA, et al. The  
182 human mitochondrial translation factor TACO1 alleviates mitoribosome stalling at polyproline  
183 stretches. *Nucleic Acids Res*. 2024;52: 9710–9726. doi:10.1093/nar/gkae645
- 184 38. Ignatov D, Shanmuganathan V, Ahmed-Begrich R, Alagesan K, Frese CK, Wang C, et al.  
185 Novel RNA-binding protein YebC enhances translation of proline-rich amino acid stretches in  
186 bacteria. *bioRxiv*. 2024; 2024.08.26.607280. doi:10.1101/2024.08.26.607280
- 187 39. Qi LS, Larson MH, Gilbert LA, Doudna JA, Weissman JS, Arkin AP, et al. Repurposing  
188 CRISPR as an RNA-guided platform for sequence-specific control of gene expression. *Cell*.  
189 2013;152: 1173–1183. doi:10.1016/j.cell.2013.02.022
- 190 40. Peters JM, Colavin A, Shi H, Czarny TL, Larson MH, Wong S, et al. A Comprehensive,  
191 CRISPR-based Functional Analysis of Essential Genes in Bacteria. *Cell*. 2016;165: 1493–1506.  
192 doi:10.1016/j.cell.2016.05.003
- 193 41. Zhang Y, Lin J, Gao Y. In silico identification of a multi-functional regulatory protein  
194 involved in Holliday junction resolution in bacteria. *BMC Syst Biol*. 2012;6 Suppl 1: S20.  
195 doi:10.1186/1752-0509-6-S1-S20
- 196 42. Choi E, Huh A, Hwang J. Novel rRNA transcriptional activity of NhaR revealed by its  
197 growth recovery for the bipA-deleted *Escherichia coli* at low temperature. *Front Mol Biosci*.  
198 2023;10: 1175889. doi:10.3389/fmolb.2023.1175889
- 199 43. Wei L, Wu Y, Qiao H, Xu W, Zhang Y, Liu X, et al. YebC controls virulence by activating  
200 T3SS gene expression in the pathogen *Edwardsiella piscicida*. *FEMS Microbiol Lett*. 2018;365.  
201 doi:10.1093/femsle/fny137

- 202 44. Hersch SJ, Wang M, Zou SB, Moon K-M, Foster LJ, Ibba M, et al. Divergent protein motifs  
203 direct elongation factor P-mediated translational regulation in *Salmonella enterica* and  
204 *Escherichia coli*. *mBio*. 2013;4: e00180-00113. doi:10.1128/mBio.00180-13
- 205 45. Elgamal S, Katz A, Hersch SJ, Newsom D, White P, Navarre WW, et al. EF-P dependent  
206 pauses integrate proximal and distal signals during translation. *PLoS Genet*. 2014;10: e1004553.  
207 doi:10.1371/journal.pgen.1004553
- 208 46. Blaha G, Stanley RE, Steitz TA. Formation of the first peptide bond: the structure of EF-P  
209 bound to the 70S ribosome. *Science*. 2009;325: 966–970. doi:10.1126/science.1175800
- 210 47. Gamper HB, Masuda I, Frenkel-Morgenstern M, Hou Y-M. Maintenance of protein  
211 synthesis reading frame by EF-P and m(1)G37-tRNA. *Nat Commun*. 2015;6: 7226.  
212 doi:10.1038/ncomms8226
- 213 48. Glick BR, Chládek S, Ganoza MC. Peptide bond formation stimulated by protein  
214 synthesis factor EF-P depends on the aminoacyl moiety of the acceptor. *Eur J Biochem*.  
215 1979;97: 23–28. doi:10.1111/j.1432-1033.1979.tb13081.x
- 216 49. Hoffer ED, Hong S, Sunita S, Maehigashi T, Gonzalez RL, Whitford PC, et al. Structural  
217 insights into mRNA reading frame regulation by tRNA modification and slippery codon-  
218 anticodon pairing. *Elife*. 2020;9: e51898. doi:10.7554/eLife.51898
- 219 50. Hubble KA, Henry MF. DPC29 promotes post-initiation mitochondrial translation in  
220 *Saccharomyces cerevisiae*. *Nucleic Acids Res*. 2023;51: 1260–1276. doi:10.1093/nar/gkac1229
- 221 51. Katz A, Solden L, Zou SB, Navarre WW, Ibba M. Molecular evolution of protein-RNA  
222 mimicry as a mechanism for translational control. *Nucleic Acids Res*. 2014;42: 3261–3271.  
223 doi:10.1093/nar/gkt1296
- 224 52. Koo B-M, Kritikos G, Farelli JD, Todor H, Tong K, Kimsey H, et al. Construction and  
225 Analysis of Two Genome-Scale Deletion Libraries for *Bacillus subtilis*. *Cell Syst*. 2017;4: 291-  
226 305.e7. doi:10.1016/j.cels.2016.12.013
- 227 53. Schindelin J, Arganda-Carreras I, Frise E, Kaynig V, Longair M, Pietzsch T, et al. Fiji: an  
228 open-source platform for biological-image analysis. *Nat Methods*. 2012;9: 676–682.  
229 doi:10.1038/nmeth.2019
- 230 54. Middleton R, Hofmeister A. New shuttle vectors for ectopic insertion of genes into  
231 *Bacillus subtilis*. *Plasmid*. 2004;51: 238–245. doi:10.1016/j.plasmid.2004.01.006
- 232 55. Camacho C, Coulouris G, Avagyan V, Ma N, Papadopoulos J, Bealer K, et al. BLAST+:  
233 architecture and applications. *BMC Bioinformatics*. 2009;10: 421. doi:10.1186/1471-2105-10-  
234 421
- 235 56. Price MN, Dehal PS, Arkin AP. FastTree 2 – Approximately Maximum-Likelihood Trees for  
236 Large Alignments. *PLOS ONE*. 2010;5: e9490. doi:10.1371/journal.pone.0009490
- 237 57. Prince CR, Lin IN, Feaga HA. The evolution and functional significance of the  
238 programmed ribosomal frameshift in prfB. *bioRxiv*. 2024; 2024.09.24.614795.  
239 doi:10.1101/2024.09.24.614795
- 240 58. Schliep KP. phangorn: phylogenetic analysis in R. *Bioinformatics*. 2011;27: 592–593.  
241 doi:10.1093/bioinformatics/btq706
- 242 59. Schoch CL, Ciufo S, Domrachev M, Hotton CL, Kannan S, Khovanskaya R, et al. NCBI  
243 Taxonomy: a comprehensive update on curation, resources and tools. *Database (Oxford)*.  
244 2020;2020: baaa062. doi:10.1093/database/baaa062
- 245 60. Shen W, Ren H. TaxonKit: A practical and efficient NCBI taxonomy toolkit. *Journal of*  
246 *Genetics and Genomics*. 2021;48: 844–850. doi:10.1016/j.jgg.2021.03.006

- 247 61. Coleman GA, Davín AA, Mahendrarajah TA, Szánthó LL, Spang A, Hugenholtz P, et al. A  
248 rooted phylogeny resolves early bacterial evolution. *Science*. 2021;372: eabe0511.  
249 doi:10.1126/science.abe0511
- 250 62. Yu G, Smith DK, Zhu H, Guan Y, Lam TT-Y. ggtree: an r package for visualization and  
251 annotation of phylogenetic trees with their covariates and other associated data. *Methods in*  
252 *Ecology and Evolution*. 2017;8: 28–36. doi:10.1111/2041-210X.12628
- 253 63. Gaidenko TA, Kim T-J, Price CW. The PrpC serine-threonine phosphatase and PrkC kinase  
254 have opposing physiological roles in stationary-phase *Bacillus subtilis* cells. *J Bacteriol*.  
255 2002;184: 6109–6114. doi:10.1128/JB.184.22.6109-6114.2002  
256

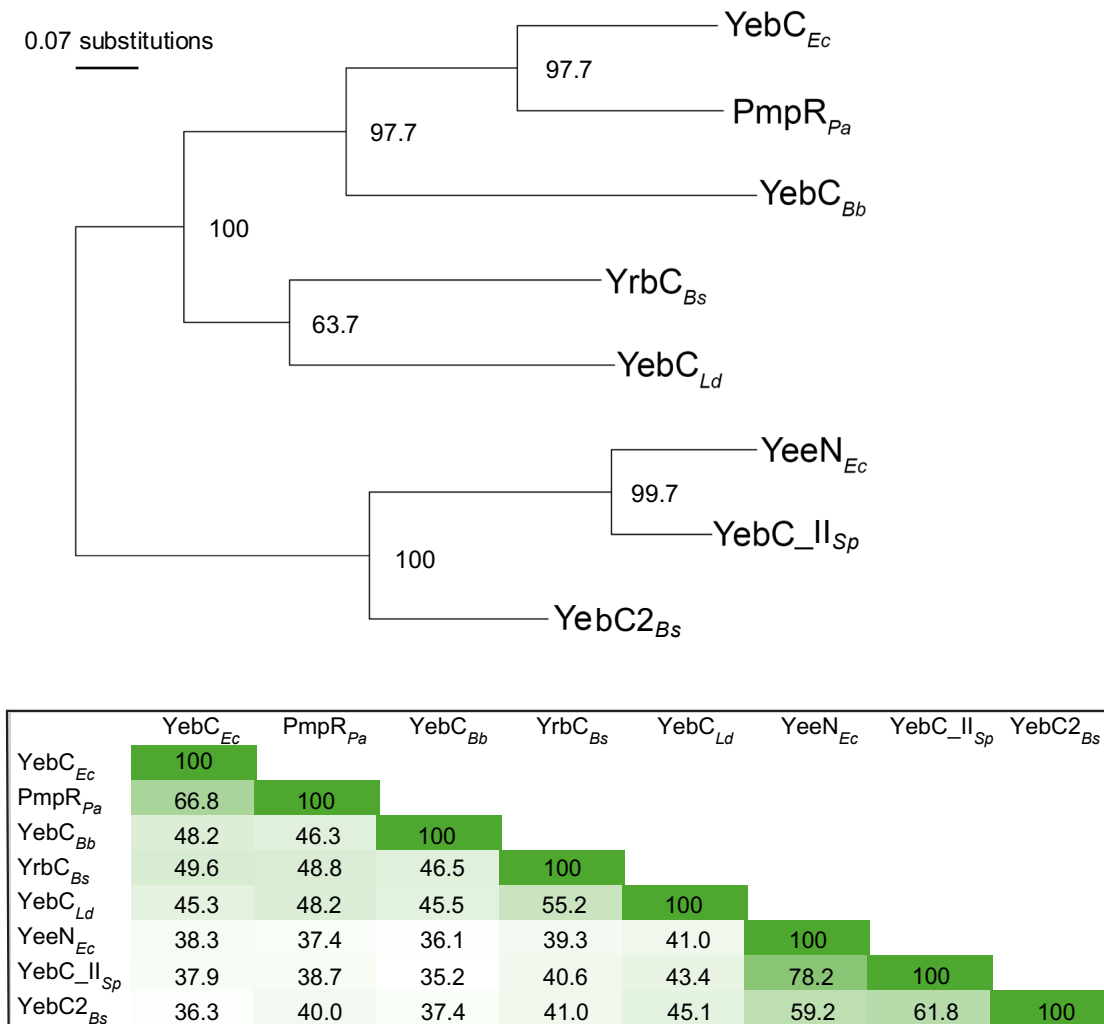
257  
258  
259



260  
261  
262  
263  
264  
265  
266

**Figure S1. His-Tagged YebC2 is functional and complements the growth defect of  $\Delta efp\Delta yebC2$  cells in vivo.** Growth curves in LB at 37°C are shown for WT,  $\Delta efp$ ,  $\Delta yebC2$ ,  $\Delta yebC2\Delta efp$  and  $\Delta yebC2\Delta efp$  expressing His-tagged YebC2.

267



268

269 **Figure S2. Midpoint rooted maximum-likelihood tree (top) and sequence similarity matrix**  
 270 **of characterized YebC family proteins (bottom).** Characterized YebC family proteins are  
 271 labelled with their given gene name and respective organism: *Bs*, *Bacillus subtilis*; *Ld*  
 272 *Lactobacillus delbrueckii*; *Pa*, *Pseudomonas aeruginosa*; *Ec*, *Escherichia coli*; *Bb*, *Borrelia*  
 273 *burgdorferi*; *Sp*, *Streptococcus pyogenes*. (Top) Bootstrap values are listed at each node.  
 274 (Bottom) Pairwise percent identities for the proteins are listed and shaded relative to their  
 275 homology.

276